Colloids and Surfaces B: Biointerfaces 171 (2018) 67–74

Contents lists available at ScienceDirect

Colloids and Surfaces B: Biointerfaces

journal homepage: www.elsevier.com/locate/colsurfb

# Monoolein liquid crystalline phases for topical delivery of crocetin

Elisabetta Esposito[a,*], Federica Carducci[b], Paolo Mariani[b], Nicolas Huang[c], Fanny Simelière[c], Rita Cortesi[a,*], Giuseppe Romeo[d], Carmelo Puglia[d]

[a] Department of Life Sciences and Biotechnologies, University of Ferrara, I-44121 Ferrara, Italy
[b] Department of Life and Environmental Sciences, Università Politecnica delle Marche, I-60131 Ancona, Italy
[c] Institut Galien Paris-Sud, CNRS, Faculté de Pharmacie, Université Paris-Sud, Univ Paris-Saclay, France
[d] Department of Drug Science, University of Catania, I-95125, Catania, Italy

ARTICLE INFO

*Keywords:*
Crocetin
Monoolein
Polarized light microscopy
Small angle x-ray scattering
Diffusion
Tape-Stripping

ABSTRACT

The present investigation concerns the production and characterization of monoolein-water systems designed for cutaneous administration of crocetin. The different monoolein crystalline phases forming in the presence of crocetin as a function of added water have been investigated by x-ray and polarized light microscopy. Franz cell was employed to compare *in vitro* the crocetin diffusion from selected monoolein water systems containing 95, 90 or 75% w/w of monoolein, while to investigate the performance of monoolein-water as transdermal delivery systems, *in vivo* studies, based on tape stripping were performed. The presence of micellar, lamellar and Q230 phases was found in the case of systems containing monoolein 95, 90 and 75% w/w respectively, with a viscosity almost directly proportional to the amount of added water. The higher the amount of water, the longer the crocetin stability, while its diffusion was slower in the case of more viscous systems. Tape stripping results indicated a more rapid depletion of crocetin on *stratum corneum* in the case of systems characterized by cubic phases, followed by micellar and lamellar ones. This behaviour could be related to a more rapid drug penetration throughout the deeper skin strata.

## 1. Introduction

Amphiphilic polar lipids, such as monoglycerides, can form various crystalline phases in the presence of different amounts of water. These lipids self-associate, depending on the temperature and aqueous content, forming reversed micellar (L2), lamellar (Lα), or bicontinuous cubic phases (C) in which the hydrocarbon chains assume a liquid-like conformation [1,2]. Particularly, glycerol monooleate (monoolein), a nontoxic, biodegradable and biocompatible material commonly used as emulsifying agent and food additive, is one of the monoglycerides most widely employed to form liquid crystalline formulations [3–5]. Different studies have attributed to monoolein a penetration enhancer activity when applied on skin, probably due to a temporary and reversible disruption of the lamellar structure of the lipid bilayer in the *stratum corneum* caused by an increase in intercellular lipid fluidity [6–8]. In the presence of tiny amounts of water (5–10%, w/w), monoolein forms reversed micelles or lamellar phases, while when more water is added (~15-40%) a cubic phase region dominates. This highly viscous isotropic phase is defined bicontinuous, being constituted of a curved three-dimensional bilayer, separating two congruent water channel networks [9,10].

Many authors have focused their attention on the relevance of the lipid crystalline phases for drug delivery [11–13]. Indeed, the presence of a lipid and an aqueous domain confers special properties to the crystalline phases, such as the ability to solubilize hydrophilic, hydrophobic, and amphiphilic substances [14–16]. In addition, liquid crystalline phases protect drugs from degradation, control drug release and possess hydrating power [17–20].

Crocetin (CRT) is an active molecule originally discovered in dried stigma of *Crocus Sativus* (Saffron), recently taken in consideration in biomedical research because of its pharmacological activities, such as antitumoral, antioxidant, antihypertensive, antiatherosclerotic and antidepressant [21–25].

In *Crocus Sativus* the chromoplast zeaxanthine cleavage dioxygenase first generates CRT dialdehyde, then converted into CRT by an aldehyde oxydo-reductase and transformed to the glucosylate derivative crocin by a glucosyl transferase [26,27]. Interestingly, recent studies have indicated the potential of CRT against skin damage induced by UV-A. Indeed, CRT reduces the oxidative stress by decreasing reactive oxygen species production and cell apoptosis [28]. Nonetheless, the antioxidant

*Abbreviations:* CRT, Crocetin; SAXS, small angle x-ray scattering

* Corresponding authors at: Department of Life Science and Biotechnology, Via Fossato di Mortara 19, I-44121 Ferrara, Italy.
*E-mail addresses:* ese@unife.it (E. Esposito), crt@unife.it (R. Cortesi).

https://doi.org/10.1016/j.colsurfb.2018.07.011
Received 11 April 2018; Received in revised form 14 June 2018; Accepted 5 July 2018
Available online 06 July 2018
0927-7765/ 

power of CRT is unfortunately associated to a low stability, especially in the presence of heat, oxygen, light and acids [29]. In the present study, monoolein-water systems have been designed and investigated as vehicles for CRT with the aim to find cutaneous systems suitable to treat skin pathologies and to protect skin against UV-induced skin damage. The different monoolein mesophases have been characterized by small angle x-ray scattering (SAXS), polarized light microscopy and rheological measurements. Tape stripping experiments enabled to shed light on the CRT distribution on stratum corneum after application of different monoolein-water systems on the skin.

## 2. Materials and methods

### 2.1. Materials

Crocin and glucosidase enzyme were purchased from Merck KGaA (Darmstadt, Germany). 2,3-Dihydroxypropyl oleate, Glyceryl monooleate, RYLO MG 19 (monoolein) was a gift from Danisco Cultor (Grindsted, Denmark). Solvents and other chemicals were purchased from Merck KGaA.

### 2.2. Preparation of crocetin

Crocetin, (2*E*,4*E*,6*E*,8*E*,10*E*,12*E*,14*E*)-2,6,11,15-Tetramethylhexadeca-2,4,6,8,10,12,14-heptaenedioic acid, CRT), was obtained in our laboratory by alkaline hydrolysis of crocin, the protocol is reported in the Supplementary materials section.

### 2.3. Production of monoolein-water samples

Monoolein based formulations were prepared by adding different amounts of water (ranging from 5 and 25% w/w) to molten monoolein at 42 °C [30,31]. When a uniform mixture was formed under stirring, the containers were sealed, to avoid water evaporation, and placed in an oven at 42 °C for 72 h. Afterwards the samples have been stirred by hand until uniform aspect. In the case of CRT containing monoolein-water systems, CRT (0.02% w/v) has been added to the samples before placing in the oven. Sample compositions and acronyms are reported in Table 1.

### 2.4. X-ray characterization

Small angle X-ray scattering (SAXS) experiments were performed at the Elettra synchrotron radiation facility (Basovizza, Trieste) at the AustroSAXS beamline. Samples were held on a flat watertight holder, to allow fixed composition studies and to avoid mechanical stress that could interfere or increase anisotropy. Experiments were performed at 37 °C on different monoolein formulations in the presence and in the absence of CRT. The investigated q-range ($q = 4\pi \sin\theta/\lambda$, where $2\theta$ is the scattering angle and $\lambda = 1.54$ Å the X ray wavelength) was 1-4 $nm^{-1}$. The observed Bragg peaks were indexed considering the different symmetries commonly observed in lipid polymorphism [32].

**Table 1**
Composition of the studied monoolein based formulations.

| Formulations | Monoolein (% w/w) | Water (% w/w) | Crocetin (% w/v)* |
|---|---|---|---|
| M-75 | 75 | 25 | – |
| M-80 | 80 | 20 | – |
| M-85 | 85 | 15 | – |
| M-90 | 90 | 10 | – |
| M-95 | 95 | 5 | – |
| M-75-CRT | 75 | 25 | 0.02 |
| M-80-CRT | 80 | 20 | 0.02 |
| M-85-CRT | 85 | 15 | 0.02 |
| M-90-CRT | 90 | 10 | 0.02 |
| M-95-CRT | 95 | 5 | 0.02 |

* With respect to the volume of the formulations.

### 2.5. Polarized light microscopy

Monoolein-water samples were examined through a polarized light microscope (Ortholux POL-MK, Carl Zeiss, Oberkochen, Germany) to verify texture and anisotropy of the liquid crystalline phases. The prepared sample was deposited on a glass slide using a spatula, to avoid any possible mechanical stress that could force the alignment of the molecules inside the sample. Once the sample was loaded, the coverslip was sealed using silicone grease, to ensure the maintenance of the monoolein hydration. For every type of formulation, three different samples were observed.

### 2.6. Rheological measurements

Rheological measurements were performed with an AR-G2 controlled-stress rotational rheometer (TA Instruments, USA). The geometry used was an aluminium cone-plate (40 mm diameter, 1° cone angle, 28 μm truncation gap). Flow curves were obtained by a flow sweep protocol: after a 2 min conditioning time, shear rate was increased from 0.1 to 2000 $s^{-1}$ for a total duration of 180 s. The temperature was maintained at 37 °C and controlled with a Peltier plate. Measurements were performed in triplicate at least for each sample, to ensure reproducibility.

### 2.7. Spreadability test

The spreading capacity of selected formulations, namely M-90 and M-95, was evaluated as follows. One hundred mg of preparation was placed on a Petri dish (3 cm diameter) and pressed by another glass dish on which a 500-g mass was positioned. Taken the time by which the formulation fills the entire dish, the following equation was used to calculate the spreadability (S) value.

$$S = m \times l / t \quad (1)$$

where m is the weight (g) tied on the upper plate, l is the diameter (cm) of the glass plate, and t is the time (s) taken for the gel to fill the entire diameter. The spreadability test was performed thrice and the mean values ± standard deviations were calculated.

### 2.8. CRT content

The content of CRT in monoolein-water systems was determined by dissolving an aliquot of sample in dimethyl sulfoxide (1:10, w/w) under magnetic stirring (ARE-6 heating magnetic stirrer, VELP Scientifica, Usmate, Italy) for 1 h in amber glass vials to avoid CRT photodegradation.

Samples were then filtered by nylon filters with 0.45 μm pore diameter (Whatman™, Germany) and finally diluted with methanol (1:10, v/v). The filtrate was then analyzed by high performance liquid chromatography (HPLC). Determinations were performed using a quaternary pump (Agilent Technologies 1200 series, USA) an UV-detector operating at 423 nm, and a 7125 Rheodyne injection valve with a 50 μl loop. Samples were loaded on a stainless-steel C-18 reverse-phase column (15 × 0.46 cm) packed with 5 μm particles (Grace® - Alltima, Alltech, USA).

Elution was performed with a mobile phase containing methanol:-water (80:20, v/v); at a flow rate of 0.8 ml/min, retention time was 3.8 min. The method was validated for linearity ($R^2 = 0.994$), repeatability (relative standard deviation 0.02%, n = 6 injections) and limit of quantification (0.03 μg/ml).

CRT content was expressed as percentage of the total amount added to monoolein-water for system production.

### 2.9. Prediction of long-term stability

The stability of CRT was assessed in stored glass containers at 40 °C for 3 months, 70–75% RH.

Chemical stability was evaluated, determining CRT content by HPLC analyses as above reported. Shelf life values were calculated as below reported [33].

Log (CRT residual content, %) was plotted against time and the slopes (m) were calculated by linear regression.

The slopes (m) were then substituted into the following equation for the determination of k values:

$$k = m \times 2.303 \quad (2)$$

Shelf life values (the time for 10% loss, $t_{90}$) and half-life (the time for 50% loss, $t_{1/2}$) were then calculated by the following equations:

$$t_{90} = 0.105/k \quad (3)$$

$$t_{1/2} = 0.693/k \quad (4)$$

### 2.10. In vitro diffusion experiments

CRT diffusion experiments were performed by Franz-type diffusion cells supplied by Vetrotecnica (Padova, Italy) associated to nylon membranes (Merck Millipore, 0.45 μm pore size).

The exposed membrane area was 0.78 $cm^2$ area (1 cm diameter orifice). The receptor compartment contained 5 ml of a mixture of phosphate buffer 60 mM pH 7.4 and ethanol (50:50, v/v). This solution was stirred with the help of a magnetic bar at 500 rpm and thermostated at 32 ± 1 °C during all the experiments [34,35].

Approximately 1 g of M-75-CRT, M-90-CRT or M-95-CRT was placed on the membrane in the donor compartment and the latter was sealed to avoid evaporation. At predetermined time intervals comprised between 0 and 24 h, samples (0.15 ml) of receptor phase solution were withdrawn and the CRT concentration in the receptor phase was measured using HPLC. Each removed sample was replaced with an equal volume of fresh receptor phase. The CRT concentrations were determined six times in independent experiments and the mean values ± standard deviations were calculated. The mean values were then plotted as a function of time. The flux coefficients were computed from the linear portion of the accumulation curve calculating the curve slopes and dividing them by the CRT concentration in the monoolein based formulation (expressed in mg/ml).

### 2.11. Tape stripping

#### 2.11.1. Volunteers recruitment

Ten volunteers of both sexes in the age range 25–55 years were recruited after medical screening, including the filling of a health questionnaire followed by physical examination of the application sites. Informed consent was obtained from all individual participants included in the study. The participants did not suffer from any ailment and were not on any medication at the time of the study. They were rested for 15 min prior to the experiments and room conditions were set at 22 ± 2 °C and 40–50% relative humidity.

#### 2.11.2. Experimental protocol

The tape stripping protocol was approved by the Ethics Committee of the University of Ferrara, Italy (study number: 170986) and conducted in accordance with the Code of Ethics of the World Medical Association (Helsinki Declaration 1964) and its later amendments for experiments involving humans.

For each subject, ten sites on the ventral surface of forearms were defined using a rectangular template (2 $cm^2$) and demarcated with permanent ink. One of the ten sites of each forearm was used as control, three sites were treated with 80 mg of M-75-CRT, three sites with 80 mg of M-90-CRT and the remaining three with 80 mg of M-95-CRT. The preparations were spread uniformly by means of a solid glass rod, thereafter the sites were occluded for 1 h using rectangular plasters especially designed for skin occlusion. Afterwards the residual formulations were removed by gently wiping with cotton balls (different for each pretreated site). Ten individual 2 $cm^2$ squares of adhesive tape (Scotch Book Tape 845, 3M) were utilized to sequentially tape-strip the *stratum corneum* on the application sites. Particularly *stratum corneum* in each pretreated site was removed at 0.5 ($t_{0.5}$), 3 ($t_3$) and 6 ($t_6$) h after formulation removal.

Each adhesive square, before and after skin tape stripping, was weighed on a semi-microbalance (sensitivity 1 mg, Sartorius model ME415S, Goettingen, Germany) to quantify the weight of removed *stratum corneum*. After each stripping, the tapes were put in the same vial containing 2 ml of the HPLC mobile phase methanol:water (80:20 v/v) and subjected to vortical stirring over 30 s. The extracted CRT was then quantified by HPLC. The recovery of CRT was validated by spiking tape-stripped samples of untreated *stratum corneum* with 2 ml of a mobile phase containing CRT 5 mg/ml [36].

#### 2.11.3. Statistical analysis

Statistical differences of *in vivo* data were determined using repeated-measures analysis of variance (ANOVA) followed by the Bonferroni-Dunn post hoc pairwise comparison procedure. The employed software was Prism 5.0, Graph Pad Software Inc. (La Jolla, CA - USA). A probability of less than 0.05 is considered significant in this study.

## 3. Results

### 3.1. Synthesis and characterization of crocetin

CRT is difficult to obtain in high yield and with a good degree of purity, thus it is hardly available commercially. For this reason, the compound was obtained in our laboratory, exploiting some experimental techniques described in Supplementary materials section.

CRT was obtained by alkaline hydrolysis, its $^1$H-NMR spectrum showed a doublet (d, $\delta = 7.21$, $J = 9.6$ Hz) and a multiplet (m, $\delta = 6.90 - 6.44$) related to hydrogens of the polyenic chain and two singlets related to hydrogens of the methyl groups placed symmetrically at the 2- and 15-positions (s, $\delta = 1.98$) and at the 6- and 11-positions (s, $\delta = 1.92$) of the chain. The $^1$H-NMR spectrum signals relative to the CRT sample coincided with those estimated by the simulation program ACD/C + H NMR Predictors (version 11.01) and with literature data [37].

### 3.2. Production of monoolein-water systems

A simple protocol was adopted to produce monoolein-water samples, notably the addition of small percentage of water to melted monoolein followed by equilibration at 42 °C resulted in transparent systems with different consistency, depending on the amount of added water (Fig S1A, Supplementary material). To assess CRT solubility, different amounts of the drug (0.2–1 mg/ml) have been added to the monoolein-water systems before equilibration at 42 °C. The transparency of the systems enabled to detect the presence of yellow crystals in the case of samples containing CRT > 0.2 mg/ml, while a homogeneous yellow colouring characterized samples with CRT 0.2 mg/ml. For all the tested monoolein-water systems the CRT content, evaluated after disaggregation and HPLC analyses, was 98% ± 0.2 with respect to the weight of CRT added to the monoolein-water mixture.

### 3.3. X-ray scattering analysis

X-ray diffraction experiments were performed to investigate the structural properties of the monoolein formulations. A few results are

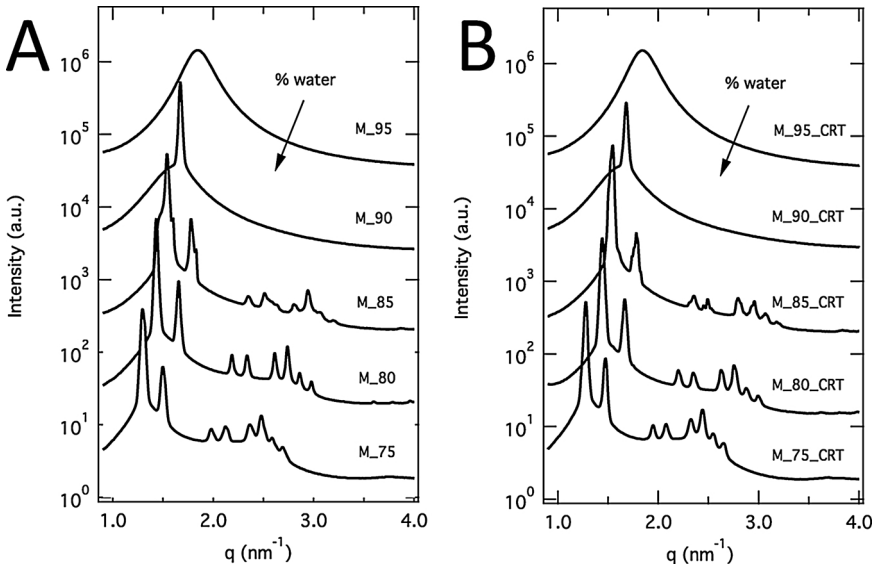


**Fig. 1.** SAXS profiles observed on monoolein, both in the absence (A) and in the presence (B) of CRT 0.02% w/v, measured at 37 °C. The black arrow indicates the direction of the increasing concentration of water. Curves were separated using offset for clarity.

**Table 2**
Macroscopic aspect, viscosity, phase symmetry and unit cell of monoolein based formulations measured at 37 °C.

| Formulations | Macroscopic aspect | Viscosity* (Pa s) ± 5% | Phase symmetry[a] | Unit cell[a] (Å) ± 0.5 |
|---|---|---|---|---|
| M-75 | gel | 1435 | cubic Ia3d (Q230) | 120.7 |
| M-80 | gel | 3514 | cubic Ia3d (Q230) | 107.4 |
| M-85 | gel | 3819 | cubic Ia3d (Q230) | 99.9 |
| M-90 | viscous | 4.6 | lamellar/micellar | 37.6 |
| M-95 | liquid | 0.3 | micellar | 34 (broad) |
| M-75-CRT | gel | 1785 | cubic Ia3d (Q230) | 118.9 |
| M-80-CRT | gel | 3224 | cubic Ia3d (Q230) | 106.7 |
| M-85-CRT | gel | 3927 | cubic Ia3d (Q230) | 99.7 |
| M-90-CRT | viscous | 5.2 | lamellar/micellar | 37.4 |
| M-95-CRT | liquid | 0.3 | micellar | 34 (broad) |

Monoolein based formulations acronyms are explained in Table 1.
* Shear rate 10 $^{s-1}$.
[a] As determined by X-ray scattering.

shown in Fig. 1, while details about phase symmetry and unit cell values are reported in Table 2.

The X-ray diffraction scattering profiles for M-95 and M-95-CRT samples show a large band centered at about 1.8 nm-1. In good agreement with the monoolein-water phase diagrams [32,38], the large band confirms the presence of a micellar phase in both systems. A narrow peak is indeed overlapped on this band in the case of the more hydrated M-90 and M-90-CRT samples, indicating the formation of the lamellar phase. For higher water concentrations, several Bragg peaks are observed; both in the absence and in the presence of CRT, the spacing of the reflections has been indexed considering the space group Q230. The characteristic profile then indicates the formation of the cubic Ia3d phase in the more hydrated conditions investigated. A schematic representation of the different lyotropic phases observed in the present systems is reported in Fig S1B (Supplementary material). It should be mentioned that the Ia3d cubic phase is bicontinuous and exhibits two 3-D networks of connected aqueous rods, co-planarly joined 3 by 3 [39].

Notably, no differences in the X-ray diffraction profiles are detected in the presence of CRT, disregarding the case of M-85-CRT sample. In this latest case, Bragg peaks appear doubled, probably due to a low homogeneity of the sample, whose concentration corresponds to the lamellar-to-Ia3d cubic phase boundary. Thus, CRT does not modify the structural organization of monoolein. Slight changes have been however detected in the unit cell parameters, which appear to be systematically reduced in the presence of CRT (Table 2), suggesting a small dehydration of the lipid layer.

### 3.4. Polarized light microscopy characterization

Polarized light microscopy enables to easily characterize the sample quality and to screen the lyotropic liquid crystalline phases in lipid-water systems. Indeed, lamellar and hexagonal phases evidence birefringence textures, as real crystals, while lack of birefringence indicates that the phase is cubic or liquid [40]. Fig. 2 shows polarized light microscopy images of M-85-CRT and M-90-CRT samples. In the case of M-85-CRT (Fig. 1A), birefringent anisotropic textures can be appreciated, probably because of the presence of phase coexistence. Instead, in the case of M-90-CRT (Fig. 1B) as well as M-95-CRT (not shown), flower-like structures typical of a lamellar phase organization can be observed [41]. Similar images were taken in the case of samples produced in the absence of CRT. In the case of the other more hydrated monoolein-water systems (from 85% to 75%), no textures have been detected, confirming the presence of a cubic phase.

### 3.5. Rheological analysis

Rheology gives valuable information about the lipid crystalline

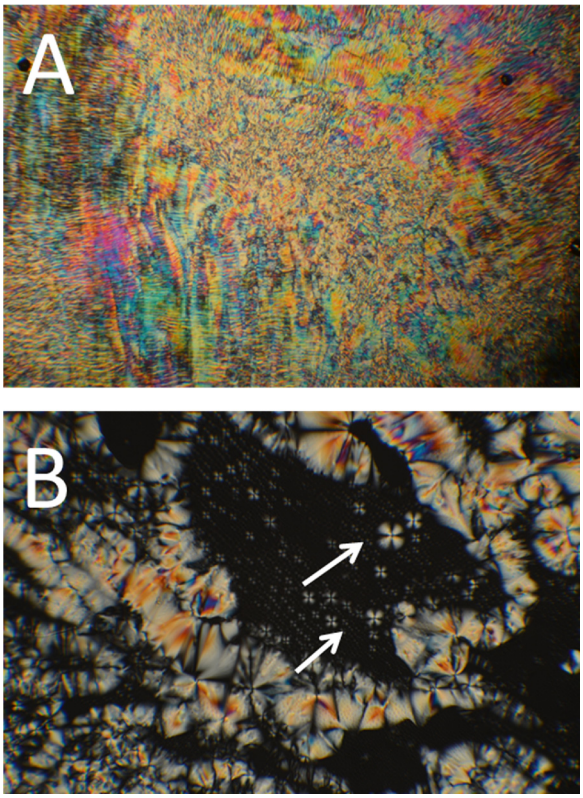


**Fig. 2.** Polarized light microscopy images of M-85-CRT (A), and M-90-CRT (B). Observations were made using a magnification 10×.

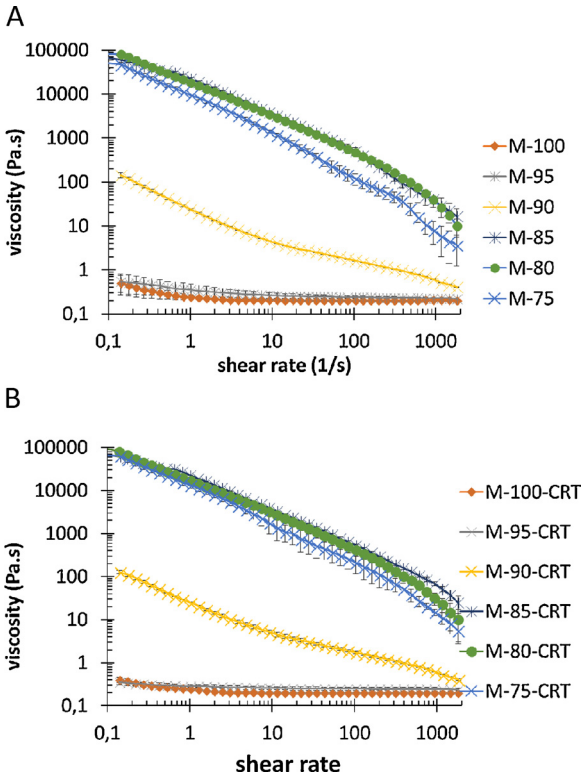


**Fig. 3.** Rheological flow curves of the indicated monoolein based formulations produced in the absence (A) or in the presence (B) of CRT. Measurements were performed at 37 °C. The geometry used was an aluminium cone-plate. Flow curves were obtained by increasing the shear rate from 0.01 $s^{-1}$ to 5000 $s^{-1}$ with 5 points per decade, each point was maintained for a duration of 180 s to perform measurements in the permanent regime. Data are the means of 3 analyses on different batches of the same type of formulations.

phases [42–44]. A comprehensive rheological characterization can be very useful for their practical applications and for the development of suitable formulations.

Results of rheological measurements performed on plain monoolein and on monoolein-water systems, in the absence or in the presence of CRT, are shown in Fig. 3, while viscosity values measured at 10 $s^{-1}$ are reported in Table 2.

Viscosity curves show that M-90, M-85, M-80 and M-75 were strongly shear-thinning.

Indeed, for these samples an appreciable decrease of the viscosity was detectable increasing the shear rate. Generally, an increase of water led to an increase of viscosity, particularly the increase was dramatic passing from M-95 to M-90, or from M-90 to M-85. Viscosity curves of M-85 and M-80 are alike and could be not distinguishable, indeed the structure for these two samples displayed the same flow behavior. The viscosity values of M-75 are slightly smaller than M-85 and M-80. M-95 and plain monoolein, employed as control, showed a slight shear-thinning behavior at low shear rate (below ≈ 1 $s^{-1}$) and a Newtonian behavior at higher shear rates. The presence of CRT did not influence the viscosity, as indicated by superimposable profiles of Fig. 3A, 3B and viscosity data reported in Table 2. Upward and downward viscosity flow sweeps have been performed on M-80, M-90, M-95 and M-100 samples (Supplementary material, Fig. S2). The samples were all weakly thixotropic and slightly more thixotropic in the case of M-90 (Fig. S2B) at low shear rates.

### 3.6. Spreadability of monoolein-water systems

Spreadability of monoolein-water systems was studied to select the systems suitable for administration on skin. Indeed, this parameter is essential for cutaneous administration since it influences extrudability from the package, uniform application and drug therapeutic efficacy [45,46]. Among the systems, only those characterized by micellar or lamellar mesophases, i.e. M-95 and M-90, were easily spreadable (spreadability ratio M-95/M-90 1.6:1) (Table S1, Supplementary materials). Monoolein-water systems based on cubic phases were not easily spreadable, apart from M-75, characterized by a viscosity lower than M-85 and M-80. The presence of CRT did not modify the system spreadability. Noteworthily, further studies have been focused on M-95-CRT, M-90-CRT and on M-75-CRT, selected to compare the micellar, lamellar and cubic phase performances as delivery system for CRT.

### 3.7. CRT stability

To assess shelf life stability, CRT content of monoolein-water systems was determined as a function of time and expressed as percentage of the total amount used for the preparation (Fig. S3, Supplementary materials). After 3 months CRT content followed the order M-75-CRT > M-90-CRT > M-95-CRT (CRT respectively 85, 71 and 54% with respect to the drug content detected after sample preparation).

**Table 3**
Shelf life data and CRT fluxes from the indicated monoolein based formulations.

| Formulations | m[a] | k[b] | $t_{90}$[b](days) | $t_{1/2}$[b](days) | flux[c] (cm/h*$10^3$) |
|---|---|---|---|---|---|
| M-75-CRT | −0.0007 | 0.0017 | 58.67 | 389.32 | 2.37 |
| M-90-CRT | −0.0016 | 0.0036 | 28.37 | 187.29 | 3.67 |
| M-95-CRT | −0.0027 | 0.0063 | 16.51 | 109.1 | 4.37 |

Monoolein based formulations acronyms are explained in Table 1.

[a] Slope of the line of log (CRT residual content %) kinetic, calculated as the mean of 3 independent determinations, s.d. ≤ 2%.

[b] K, $t_{90}$ and $t_{1/2}$ were calculated following Eqs. (1), (2) and (3) respectively.

[c] Calculated by Franz cell experiment, considering the slope of the line of CRT diffusion and its concentration in the monoolein formulations.

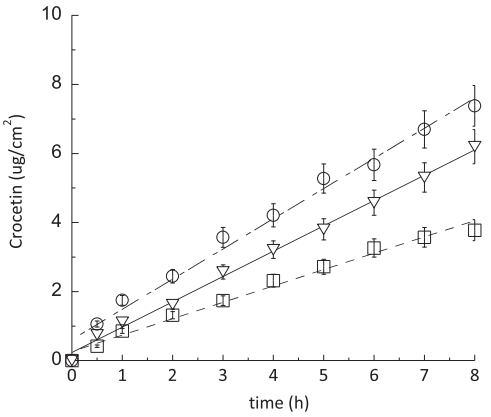


**Fig. 4.** In vitro diffusion profiles of CUR from M-75-CRT (squares), M-90-CRT (circles) and M-95-CRT (crosses). Experiments were performed by Franz cell associated to nylon membranes. Data represent the mean of six independent experiments ± S.D.

Table 3 reports shelf life ($t_{90}$) and half-life ($t_{1/2}$) values calculated by Eqs. (2) and (3).

It was found that $t_{1/2}$ value of CRT exceeded 1 year in the case of M-75-CRT, 6 months in the case of M-90-CRT and 3 months in the case of M-95-CRT. All data were statistically significant ($p < 0.0001$).

All monoolein/water systems maintained their physical appearance with time, without phase separation phenomena also after six months from production.

### 3.8. In vitro CRT diffusion

The diffusion of CRT included in M-75-CRT, M-90-CRT and M-95-CRT was compared by Franz cell experiments. Notably the receptor phase was constituted of a phosphate buffer/ethanol 50:50 (v/v) mixture to allow the establishment of the sink conditions and to sustain permeant solubilization [34]. Fig. 4 shows the diffusion kinetics corresponding to the linear part of the profile (from 0 to 8 h), while the flux values are reported in Table 3. The diffusion of CRT was more controlled in the case of M-75-CRT with respect to the other forms. Indeed, M-75-CRT flux value was almost half than M-95-CRT and 2/3 with respect to M/90-CRT.

### 3.9. Tape-stripping evaluation

A monocentric observational experiment was conducted by tape stripping for quantifying CRT presence in the *stratum corneum* after cutaneous administration of M-75-CRT, M-90-CRT and M-95-CRT [36,47]. Formulations have been applied on the forearms following the scheme depicted in data in Supplementary material Fig. S4. Portions of *stratum corneum* have been stripped at $t_{0.5}$, $t_3$ and $t_6$. Tape stripping results are summarized in Fig. 5. A general depletion in the amount of CRT in the *stratum corneum* was observed by time. Notably, in the case of M-75-CRT, the CRT amount at $t_{0.5}$ was 3.5 and 2-fold higher with respect to M-90-CRT and M-95-CRT respectively (Fig. 5A). Fig. 5B shows a comparative evaluation of the CRT level present in *stratum corneum* at $t_3$ and $t_6$ with respect to $t_{0.5}$. A depletion of CRT more pronounced in the case of M-75-CRT was observed, followed by M-90-CRT and M-95-CRT (Fig. 5B). The CRT amounts detected in the *stratum corneum* at $t_{0.5}$ and $t_3$ were significantly different. The extraction efficiency of CRT was 97.8 ± 0.4% (n = 3).

## 4. Discussion and conclusions

The powerful activity of CRT makes this molecule interesting both for pharmaceutical, as well as for cosmeceutical applications. We

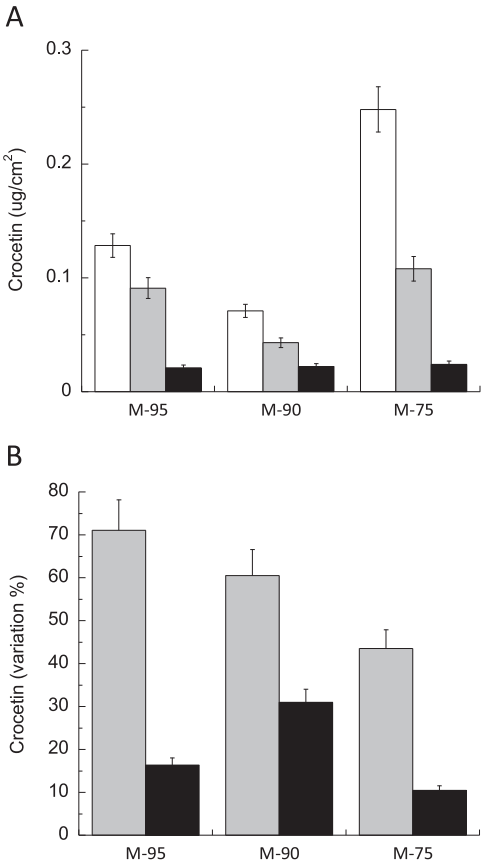


**Fig. 5.** Tape stripping evaluation. A: CRT amount in the *stratum corneum* after M-90-CRT, M-95-CRT and M-75-CRT application, removal and tape stripping. Tape stripping was performed $t_{0.5}$ (white), $t_3$ (light) and $t_6$ (dark) from formulation removal. B: comparative evaluation of the CRT level present at $t_3$ (light bars) and $t_6$ (dark bars) in *stratum corneum*. The reported levels represent the percentage of CRT with respect to that present in *stratum corneum* at $t_{0.5}$. Data represent the mean for ten subjects ± S.D., $p < 0.001$.

succeeded to obtain this molecule by alkaline hydrolysis of crocin. To find vehicles able to solubilize and deliver CRT through the skin, monoolein-water systems were investigated. In these captivating systems, monoolein disposes in various forms as a function of water content, resulting in different crystalline mesophases. SAXS characterization of monoolein water-systems enabled to identify micellar, lamellar or Q 230 phases. Namely these latest mesophases were found for 15–25 % water content. These results confirm previously findings of other authors and agree well with polarized light microscopy observations and rheological measurements [30,43,44]. Indeed, birefringence of M-90, M-90-CRT, M-95 and M-95-CRT samples allowed to observe flower-like structures typical of lamellar phases, while samples with 20–25 % water content did not transmit the light, being characterized by isotropic cubic phases.

Viscosity profiles are very intriguing, indeed monoolein-water samples showed a non-continuous behavior under dilution (Fig. 3A and B). Namely, an almost Newtonian behavior was observed for 0–5% water content, while samples containing 10–25 % of water were strongly shear-thinning, suggesting an important structure rearrangement under shear. Such viscosity behavior can be directly related to the structure of the various monoolein phases, having a different degree of entanglement. Indeed, the disordered isotropic micellar phase (M-95), occurring in very dehydrated conditions, was very fluid (viscosity < 1 Pa s), while an increase of water concentration led to lamellar phase formation (M-90), characterized by a 1-D ordered structure and a dramatically higher viscosity (1–100 Pa s). A second remarkable change in viscosity (100–100000 Pa s) was observed in the case of cubic Ia3d

phase, showing a 3-D ordered structure, thus particularly viscous. Notably, viscosity values of samples in the Ia3d cubic phase (M-85, M-80 and M-75) slightly decreased, as a function of water content. It can be suggested that under hydration the cubic phase softens because of the changes in the monoolein structural parameters. Indeed, with the same degree of entanglement, the lipid bilayer curvature, the area-per-molecule at the lipid/water interface and the hydrocarbon chain packing should play a key role on the mechanical properties of the phase [32].

Regarding chemical stability, monoolein-water systems preparation did not induce degradation of CRT, as indicated by HPLC analyses of systems after sample disaggregation.

Shelf life and Franz cell studies evidenced that the system characterized by cubic phases better controlled stability and diffusion of CRT with respect to micellar and lamellar based systems. These differences could be attributed both to the viscosity and to the crystallographic structure of the systems, indeed, the viscosity of liquid crystalline phases can affect the diffusion kinetics of the solubilized active molecules. Notably, the bicontinuous cubic phases are more rigid than the lamellar ones, described as plastic fluids undergoing yielding [43,44].

Tape stripping experiments enabled to shed light on the performance of monoolein mesophases as cutaneous delivery systems for CRT. At the first-time interval ($t_{0.5}$), the higher CRT amount found in *stratum corneum* in the case of M-75-CRT could account for its higher viscosity that could initially prolong its permanence on skin with respect to M-90-CRT and M-95-CRT. It should be considered that monoolein can alter the skin barrier properties due to interactions with the intercellular lipids in the *stratum corneum*. These alterations of lipid packing lead to hydration of stratum corneum and disorganization of the lipid bilayers [7,18]. At $t_3$ and $t_6$, it is noteworthy that the CRT depletion was not ascribable to high monoolein/water ratio, indeed in the case of micellar (M-95-CRT) or lamellar phases (M-90-CRT), CRT depletion was less pronounced with respect to the cubic phase system (M-75-CRT). The more pronounced depletion of CRT found in the case of M-75-CRT could be justified by the hypothesis of a penetration enhancement effect, due to an interaction between cubic phase system and *stratum corneum* lipids. This hypothesis is corroborated by some studies indicating a higher skin permeability exerted by cubic phases with respect to lamellar ones [48] while others suggested a similarity between the cubic phase structure and the structure of the stratum corneum [49]. Thus, it could be suggested that monoolein organized in cubic mesophases could mix with *stratum corneum* lipids and induce an intercellular lipid disorder, finally promoting skin uptake.

On the other hand, it can be asserted that the lower viscosity of M-90-CRT and M-95-CRT initially promotes CRT penetration through *stratum corneum* ($t_{0.5}$), afterwards the drug is slowly subtracted, suggesting the formation of a monoolein depot within the *stratum corneum* lipids. At this regard, it should be considered that CRT should long remain in the upper skin strata to exert its skin protection against UV damage, thus a prolong permanence is desirable, while a deeper CRT penetration should be avoided. Moreover, it is noteworthy that rheological properties (shear-thinning behaviour) and spreadability of the lamellar phase make it more appropriate for cutaneous application with respect to the cubic one.

Eventually this study has demonstrated the suitability of monoolein-water systems as cutaneous vehicles for CRT, nonetheless further in vivo studies are needed (i) to verify the antioxidant activity and skin protection of the different CRT containing systems, (ii) to point out the mechanism of monoolein mesophases and CRT distribution in the different skin layers.

## Conflict of interest

The authors declare that there is no conflict of interests.

## Acknowledgements

The authors are grateful to Maddalena Sguizzato and Debora Santonocito for conducting in vitro diffusion experiments and CRT synthesis.

## Appendix A. Supplementary data

Supplementary material related to this article can be found, in the online version, at doi: https://doi.org/10.1016/j.colsurfb.2018.07.011.

## References

[1] J.M. Seddon, R.H. Templer, Polymorphism of lipid-water systems, in: R. Lipowsky, E. Sackmann (Eds.), Handbook of Biological Physics, vol. 1, Elsevier Science Publishers B.V., N.Y., United States, 1995.
[2] R. Mezzenga, Physics of self-assembly of lyotropic liquid crystals, in: Nissim Garti, Ponisseril Somasundaran, Raffaele Mezzenga (Eds.), Self-Assembled Supramolecular Architectures: Lyotropic Liquid Crystals, John Wiley & Sons Inc, Hoboken, New Jersey, 2012, pp. 19–35 edited by.
[3] A. Ganem-Quintanar, D. Quintanar-Guerrero, P. Buri, Monoolein: a review of the pharmaceutical applications, Drug. Dev. Ind. Pharm. 26 (2000) 809–820.
[4] P. Mariani, F. Rustichelli, L. Saturni, Cordone L, Stabilization of the monoolein Pn3m cubic structure on trehalose glasses, Eur. Biophys. J. 28 (1999) 294–301.
[5] V. Chandrashekhar, W.W. Kulkarni, I.-S. Guillermo, S. Engelskirchen, S. Ahuallia, Monoolein: a magic lipid? Phys. Chem. Chem. Phys. 13 (2011) 3004–3021.
[6] L.B. Lopes, J.H. Collett, M.V. Bentley, Topical delivery of cyclosporin A: an in vitro study using monoolein as a penetration enhancer, Eur. J. Pharm. Biopharm. 60 (2005) 25–30.
[7] L.B. Lopes, F.F. Speretta, M. Bentley, Enhancement of skin penetration of vitamin K using monoolein-based liquid crystalline systems, Eur. J. Pharm. Sci. 32 (2007) 209–215.
[8] S. Milak, A. Zimmer, Glycerol monooleate liquid crystalline phases used in drug delivery systems, Int. J. Pharm. 478 (2015) 569–587.
[9] K. Larsson, Cubic lipid–water phases: structures and biomembrane aspects, J. Phys. Chem. 93 (1989) 7304–7314.
[10] K. Larsson, Aqueous dispersions of cubic lipid–water phases, Curr. Opin. Colloid Interface Sci. 5 (2000) 64–69.
[11] M.G. Lara, M.V.L.B. Bentley, J.H. Collett, In vitro drug release mechanism and drug loading studies of cubic phase gels, Int. J. Pharm. 293 (2005) 241–250.
[12] A.R. Ahmed, A. Dashevsky, R. Bodmeier, Drug release from and sterilization of in situ cubic phase forming monoglyceride drug delivery systems, Eur. J. Pharm. Biopharm. 75 (2010) 375–380.
[13] J.C. Shah, Y. Sadhale, D.M. Chilukuri, Cubic phase gels as drug delivery systems, Adv. Drug Deliv. Rev. 47 (2001) 229–250.
[14] A. Zabara, R. Mezzenga, Controlling molecular transport and sustained drug release in lipid-based liquid crystalline mesophases, J. Control. Release 188 (2014) 31–43.
[15] S.B. Rizwan, B.J. Boyd, T. Rades, S. Hook, Bicontinuous cubic liquid crystals as sustained delivery systems for peptides and proteins, Expert Opin. Drug Deliv. 7 (2010) 1133–1144.
[16] C. Guo, J. Wang, F. Cao, R.J. Lee, G. Zhai, Lyotropic liquid crystal systems in drug delivery, Drug Discov. Today 15 (2010) 1032–1040.
[17] H. Evenbratt, A. Strom, Phase behavior, rheology, and release from liquid crystalline phases containing combinations of glycerol monooleate, glyceryl monooleyl ether, propylene glycol, and water, RSC Adv. 7 (2017) 32966–32973.
[18] L.B. Lopes, F.F. Speretta, M.V. Bentley, Enhancement of skin penetration of vitamin K using monoolein-based liquid crystalline systems, Eur. J. Pharm. Sci. 32 (2007) 209–215.
[19] I. Amar-Yuli, D. Libster, A. Aserin, N. Garti, Solubilization of food bioactives within lyotropic liquid crystalline mesophases, Curr. Opin. Colloid Interface Sci. 14 (2009) 21–32.
[20] F. Caboi, G.S. Amico, P. Pitzalis, M. Monduzzi, T. Nylander, K. Larsson, Addition of hydrophilic and lipophilic compounds of biological relevance to the monoolein/water system. Phase behaviour, Chem. Phys. Lipids 109 (2001) 47–62.
[21] S.Z. Bathaie, R. Hoshyar, H. Miri, M. Sadeghizadeh, Anticancer effects of crocetin in both human adenocarcinoma gastric cancer cells and rat model of gastric cancer, Biochem. Cell Biol. 91 (2013) 397–403.
[22] F. Yoshino, A. Yoshida, N. Umigai, K. Kubo, M.C. Lee, Crocetin reduces the oxidative stress induced reactive oxygen species in the stroke-prone spontaneously hypertensive rats (SHRSPs) brain, J. Clin. Biochem. Nutr. 49 (2011) 182–187.
[23] E. Christodoulou, N.P. Kadoglou, N. Kostomitsopoulos, G. Valsami, Saffron: a natural product with potential pharmaceutical applications, J. Pharm. Pharmacol. 67 (2015) 1634–1649.
[24] M. Giaccio, Crocetin from saffron: an active component of an ancient spice, Crit. Rev. Food Sci. Nutr. 44 (2004) 155–172.
[25] L. Song, C. Kang, Y. Sun, W. Huang, W. Liu, Z. Qian, Crocetin inhibits lipopolysaccharide- induced inflammatory response in human umbilical vein endothelial cells, Cell Physiol. Biochem. 40 (2016) 443–452.
[26] F. Bouvier, C. Suire, J. Mutterer, B. Camara, Oxidative remodeling of chromoplast carotenoids: identification of the carotenoid dioxygenase CsCCD and CsZCD genes involved in Crocus secondary metabolite biogenesis, Plant Cell. 15 (2003) 47–62.
[27] O. Ahrazem, A. Rubio-Moraga, J. Berman, T. Capell, P. Christou, C. Zhu, L. Gómez-

Gómez, The carotenoid cleavage dioxygenase CCD2 catalysing the synthesis of crocetin in spring crocuses and saffron is a plastidial enzyme, New Phytol. 209 (2016) 650–663.
[28] T. Ohba, M. Ishisaka, S. Tsujii, K. Tsuruma, M. Shimazawa, K. Kubo, N. Umigai, T. Iwawaki, H. Hara, Crocetin protects ultraviolet A-induced oxidative stress and cell death in skin in vitro and in vivo, Eur. J. Pharmacol. 789 (2016) 244–253.
[29] M. Tsimidou, E. Tsatsaroni, Stability of saffron pigments in aqueous extracts, J. Food Sci. 58 (1993) 1073–1075.
[30] P. D'Antona, W.O. Parker, M.C. Zanirato, E. Esposito, C. Nastruzzi, Rheological and NMR characterization of monoglyceride-based formulations, J. Biomed. Mater. Res. 52 (2000) 40–52.
[31] E.Esposito.V. Carotta, A. Scabbia, L. Trombelli, P. D'Antona, E. Menegatti, C. Nastruzzi, Comparative analysis of tetracycline-containing dental gels: poloxamer- and monoglycerides-based formulations, Int. J. Pharm. 142 (1996) 9–23.
[32] S. Mazzoni, L.R.S. Barbosa, S.S. Funari, R. Itri, P. Mariani, Cytochrome-c affects the monoolein polymorphism: consequences for stability and loading efficiency of drug delivery systems, Langmuir 32 (2016) 873–881.
[33] A. Garg, D. Aggarwal, S. Garg, A.K. Singla, Spreading of semisolid formulations. An update, Pharm. Technol. 26 (2002) 84–105.
[34] W.J. Pugh, Kinetics of product stability, in: M.E. Aulton (Ed.), Aultons´s Pharmaceutics. The Design and Manufacture of the Medicines, 3rd ed., Churchil Livingstone Elsevier, London, 2007, pp. 99–107.
[35] M. Siewert, J. Dressman, C.K. Brown, V.P. Shah, FIP/AAPS guidelines to dissolution/in vitro release testing of novel/special dosage forms, AAPS PharmSciTech 4 (2003) E7.
[36] L.M. Andrade, C. de Fátima Reis, L. Maione-Silva, J.L.V. Anjos, A. Alonso, Rl.C. Serpa, R.N. Marreto, E.M. Lima, S.F. Taveira, Impact of lipid dynamic behavior on physical stability, in vitro release and skin permeation of genistein-loaded lipid nanoparticles, Eur. J. Pharm. Biopharm. 88 (2014) 40–47.
[37] E. Esposito, M. Sguizzato, M. Drechsler, P. Mariani, F. Carducci, C. Nastruzzi, Cortesi R, Progesterone lipid nanoparticles: scaling up and in vivo human study, Eur. J. Pharm. Biopharm. 119 (2017) 437–446.
[38] M.-R. Van Calsteren, M.C. Bissonnette, F. Cormier, C. Dufresne, T. Ichi, J.C.Y. LeBlanc, D. Perreault, I. Roewer, Spectroscopic characterization of crocetin derivatives from Crocus sativus and Gardenia jasminoides, J. Agric. Food Chem. 45 (1997) 1055–1061.
[39] J. Briggs, H. Chung, M. Caffrey, The temperature-composition phase diagram and mesophase structure characterization of the monoolein/water system, J. Phys. II, EDP Sci. 6 (1996) 723–751.
[40] P. Mariani, V. Luzzati, H. Delacroix, Cubic phases of lipid-containing systems. Structure analysis and biological implications, J. Mol. Biol. 204 (1988) 165–189.
[41] C.C. Muller-Goymann, Physicochemical characterization of colloidal drug delivery systems such as reverse micelles, vesicles, liquid crystals and nanoparticles for topical administration, Eur. J. Pharm. Biopharm. 58 (2004) 343–356.
[42] Y. Iwashita, H. Tanaka, Self-organization in phase separation of a lyotropic liquid crystal into cellular, network and droplet morphologies, Nat. Mater. 5 (2006) 147–152.
[43] L. Sagalowicz, M. Michel, M. Adrian, P. Frossard, M. Rouvet, H.J. Watzke, A. Yaghmur, L. de Campo, O. Glatter, M.E. Leser, Crystallography of dispersed liquid crystalline phases studied by cryo-transmission electron microscopy, J. Microsc. 221 (2006) 110–121.
[44] E. Esposito, M. Sguizzato, C. Bories, C. Nastruzzi, R. Cortesi, Production and characterization of clotrimazole liposphere gel for candidiasis treatment, Polymers 10 (2018) 160–175.
[45] E. Esposito, M. Drechsler, N. Huang, G. Pavoni, R. Cortesi, D. Santonocito, C. Puglia, Ethosomes and organogels for cutaneous administration of crocin, Biomed. Microdevices 18 (2016) 1–12.
[46] R. Mezzenga, C. Meyer, C. Servais, A.I. Romoscanu, L. Sagalowicz, R.C. Hayward, Shear rheology of lyotropic liquid crystals: a case study, Langmuir 21 (2005) 3322–3333.
[47] G. Bonacucina, G.F. Palmieri, D.Q.M. Craig, Rheological and dielectric characterization of monoolein/water mesophases in the presence of a peptide drug, J. Pharm. Sci. 94 (2005) 2452–2462.
[48] D.G. Lim, W.-W. Jeong, N.A. Kim, J.Y. Lim, S.-H. Lee, W.S. Shim, N.-G. Kang, S.H. Jeong, Effect of the glyceryl monooleate-based lyotropic phases on skin permeation using in vitro diffusion and skin imaging, Asian J. Pharm. Sci. 9 (2014) 324–329.
[49] N. Lars, A.-A. Ashraf, Stratum corneum keratin structure, function, and formation: the cubic rod-packing and membrane templating model, J. Invest. Dermatol. 4 (2004) 715–732.